

Anelastic relaxation due to clustered self-interstitial atoms in Al

K.-H. Robrock, L. E. Rehn,* V. Spirić, and W. Schilling

Institut für Festkörperforschung der Kernforschungsanlage Jülich, D 517 Jülich, Germany

(Received 10 May 1976)

Anelastic processes in Al single crystals present after low-temperature electron irradiation have been investigated using both internal-friction and elastic-aftereffect techniques. Several stress-induced relaxation processes have been observed, one due to the I_B close-pair defect, and six others attributed to small interstitial clusters formed during long-range interstitial migration in recovery stage I. Details are presented concerning the creation, stability, symmetry, and relaxation kinetics of the various defects responsible for the anelastic processes. One of the processes exhibits all the characteristics expected for a configuration of the di-interstitial proposed by Johnson. A model is discussed which suggests how a small interstitial cluster may undergo reorientation without simultaneous migration of the defect center of mass.

I. INTRODUCTION

In the preceding paper,¹ we discussed in detail our observations of an anelastic relaxation effect (called process A) due to the stress-induced reorientation of single self-interstitial atoms (SIA's) in aluminum. The present paper continues the description of anelastic relaxation phenomena found in low-temperature electron-irradiated aluminum single crystals. It will be shown that several additional anelastic effects occur, one due to I_B close-pair defects, and at least six others caused by the stress-induced reorientation of small interstitial clusters. These clusters are formed during migration of the single SIA's in annealing stage I. In stage II, the smaller clusters disappear, and the average number of SIA's per cluster increases.² Understanding of the clustering process is important, because it is responsible for the retention of a considerable portion of the irradiation-produced damage above temperatures where defect mobility first occurs.

The ability of anelastic measurements to discriminate between different types of clusters present simultaneously in a sample is particularly helpful in the study of interstitial clustering. Although it is not possible on the basis of the present measurements to identify uniquely the various cluster configurations which are formed, it is possible to observe the growth and decay of particular types, and to extract information about their symmetry, stability, and relaxation kinetics.

An important difference exists between two of the observed processes (A and B), which are attributed to the initial two steps in the formation of interstitial clusters during annealing, and all the other effects which are observed. The reorientation jump in both processes A and B leads simultaneously to long-range defect migration, and therefore to reactions with other defects in the lattice. In contrast, additional processes were

found which exhibit no annealing at the peak temperature, demonstrating that the stress-induced reorientation of these defects does not lead to long-range migration. Because of their stability, it was possible to observe these processes with internal-friction measurements, as well as with the elastic-aftereffect (EAE) technique. Consequently, it was possible to make very accurate determinations of their activation energies and preexponential time constants.

A detailed description of the EAE technique and experimental arrangement is given elsewhere.^{1,3} Tubelike 99.999% pure aluminum single-crystal samples were used in an inverted torsion pendulum. The torsion axes of the samples were oriented within $\pm 3^\circ$ along a $\langle 100 \rangle$, $\langle 110 \rangle$, or $\langle 111 \rangle$ crystallographic direction. Irradiations were performed at 4.7 K with 3-MeV electrons generated by the Van de Graaff accelerator⁴ at the Kernforschungsanlage, Jülich. Defect concentrations were monitored by measuring both the diaelastic modulus change produced during irradiation,³ and the resistivity changes in two simultaneously irradiated samples. The linear decreases of the elastic moduli which occurred during irradiation showed that all dislocation segments had been effectively pinned. Following irradiation, the sample temperature was varied in a stepwise fashion, during which the anelastic processes were observed.

Internal-friction measurements were made by electromagnetically exciting the sample in torsion (at its natural frequency of about 40 Hz) to a maximum strain of about 10^{-5} , and observing the free decay. Frequency changes $\Delta f/f$ could then be determined to an accuracy of $\pm 1 \times 10^{-5}$, and changes in damping $\Delta Q^{-1}/Q^{-1}$ to about 2×10^{-4} , for $Q^{-1} < 10^{-3}$. The EAE technique was capable of resolving changes in strain as small as 5×10^{-10} . Mechanical instabilities in the cryostat, however, limited the long-term (30-min) accuracy to about

$\pm 5 \times 10^{-9}$.

The determination of defect symmetries on the basis of anelastic measurements is discussed in detail by Nowick and Berry.⁵ Measurements performed in torsion on cubic crystals are quite specific in the case of a tetragonal or $\langle 100 \rangle$ or orthorhombic defect, since an effect appears in the $\langle 111 \rangle$ orientation but not in the $\langle 100 \rangle$. All defects with lower symmetry however, may, in torsion, produce relaxation effects in all crystal orientations. Although in this case the ratio of the relaxation strengths in the two different orientations still contains information about the defect symmetry, this ratio is also a function of the magnitude of the defect anisotropy. For defect symmetries other than tetragonal or $\langle 100 \rangle$ orthorhombic, it is therefore not possible to determine uniquely the symmetry solely on the basis of such measurements.

II. RESULTS

Figure 1 provides an overview of the stable anelastic processes found in low-temperature irradiated aluminum. Here, the internal-friction results for a $\langle 110 \rangle$ -oriented crystal irradiated to a Frenkel-pair concentration of 5×10^{-4} (resistivity change of 200 n Ω cm) are shown. The different curves have been artificially shifted in a vertical direction for clarity, and were obtained in the following fashion. After irradiation, the sample

temperature was raised stepwise up to a maximum value of 45 K, and measurements of internal friction (Q^{-1}) and resonant frequency (f) were made at each indicated temperature. Then the sample was cooled to 6 K, and a second run was begun leading to a slightly higher maximum temperature (46 K) after which the sample was again cooled to 6 K. Each successive run was continued to a higher maximum temperature. In this manner, not only the existence of an internal-friction peak could be determined, but it was also possible to study the growth and annealing of certain processes. The first run (labeled ~ 25 K) was initiated after an inadvertent warming of the sample to about 25 K. This caused the annihilation of internal-friction peak 1, located at 19 K. However, this peak was found after an identical irradiation of another $\langle 110 \rangle$ sample, for which no accidental warming had occurred. These results are included in Fig. 1 as the curve labeled "After Irradiation." Six internal-friction peaks appear. Labeled according to the existing nomenclature,⁵ they are as follows: peaks 0, 1, 2, 3, 4, and 5 at about 6, 19, 43, 52, 58, and 69 K, respectively. We have also measured a corresponding decrease of the correct order of magnitude in the resonant frequency for each of these peaks, demonstrating that they all are due to a real anelastic relaxation process.

The EAE results are presented in the form of isochronal aftereffect curves¹ in Figs. 2 and 3 for

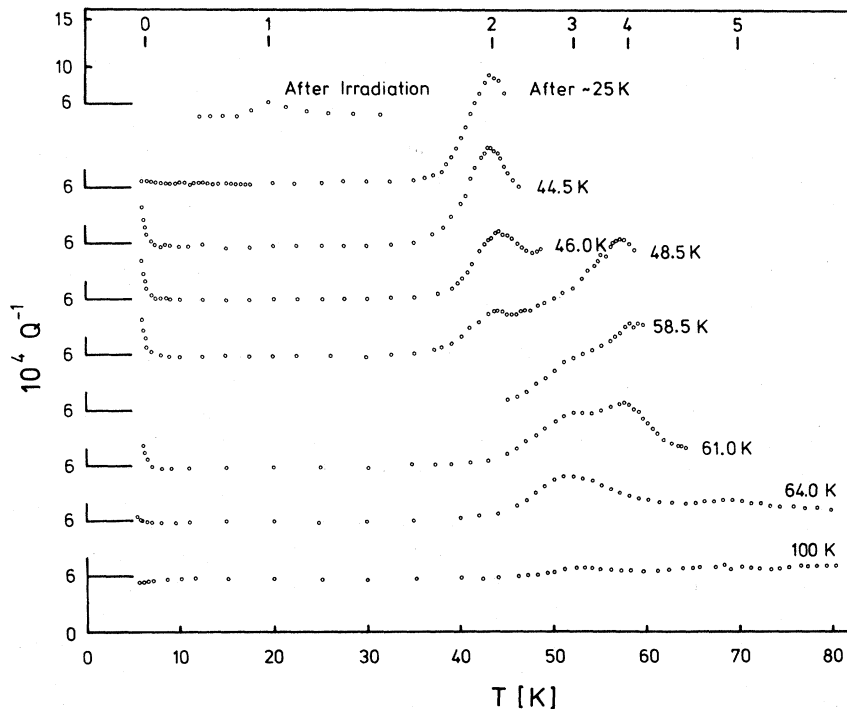


FIG. 1. Internal-friction results for a $\langle 110 \rangle$ oriented crystal irradiated to a Frenkel pair concentration of approximately 5×10^{-4} . Each curve is labeled by the maximum annealing temperature attained prior to its measurement.

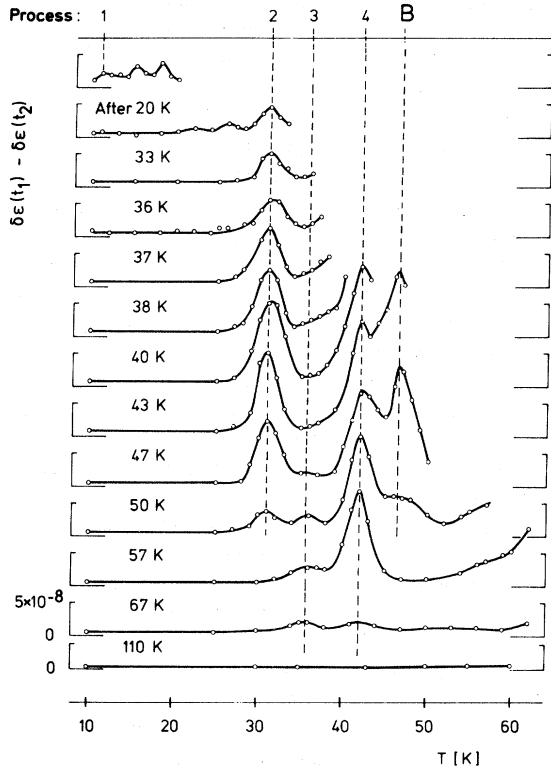


FIG. 2. Isochronal elastic-aftereffect curves for a $\langle 100 \rangle$ oriented crystal irradiated to a Frenkel-pair concentration of approximately 4×10^{-4} . Each curve is labeled by the maximum annealing temperature attained prior to its measurement.

a $\langle 100 \rangle$ and a $\langle 111 \rangle$ oriented crystal, for which the total irradiation produced resistivity changes were 170 and 270 n Ω cm, respectively. These curves show the total anelastic strain measured at the indicated temperature between 30 and 300 sec after removal of the loading stress. In all cases, the loading was of 300-sec duration, and produced an elastic strain of approximately 3×10^{-5} . One advantage of this form of presentation is that, as with the internal-friction measurements, the existence of an anelastic process manifests itself as a peak. The data points were again obtained by varying the sample temperature in a manner similar to that described above for the internal-friction measurements. Five prominent peaks, labeled 1, 2, 3, 4, and B, occur in Fig. 2. This labeling was chosen because the annealing behavior and activation energies of the EAE peaks 1-4 show that they are due to the same four anelastic processes previously labeled 1-4 in the internal-friction results. An additional peak A appears in the $\langle 111 \rangle$ crystal; it has been discussed in detail elsewhere.¹ Thus, as anticipated, all relaxation process which

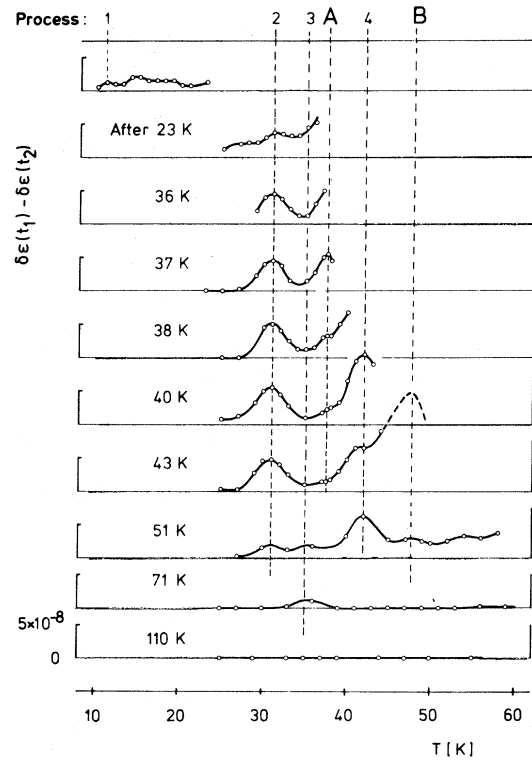


FIG. 3. Isochronal elastic-aftereffect curves for a $\langle 111 \rangle$ oriented crystal irradiated to a Frenkel-pair concentration of approximately 7×10^{-4} . Each curve is labeled by the maximum annealing temperature attained prior to its measurement.

were observed in the internal-friction study except processes 0 and 5 are again found in the EAE results. The quality of the present EAE data is further exemplified by the complete lack of any background effects ($\Delta\epsilon < 5 \times 10^{-9}$) in both sample orientations after the 110-K anneal. The absence of any anelastic contribution from the Bordoni relaxation⁵ indicates that, as expected for these irradiation doses, all dislocation segments have been pinned.

In Fig. 4, the measured relaxation times τ for processes 2, 3, 4, and B are shown in an Arrhenius plot, i.e., $\ln\tau$ versus reciprocal measuring temperature. Internal-friction measurements of fast neutron⁶ and α -particle⁷ irradiated aluminum have also been included. Since the relaxation time at the peak temperature is 100 sec in the EAE results but only about 4×10^{-3} sec in the internal-friction case, the relaxation times have been determined over almost five orders of magnitude.

In order to facilitate comparison of the anelastic results with other studies of irradiated metals, resistivity measurements were made on samples

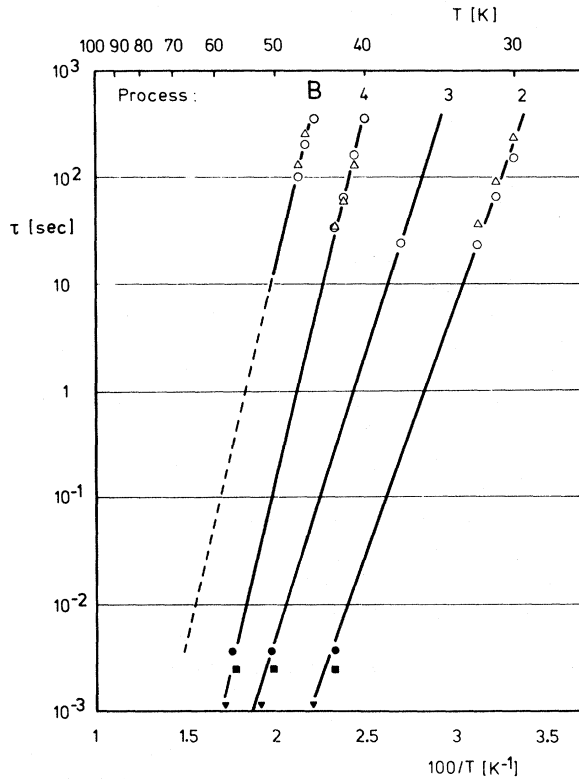


FIG. 4. Arrhenius diagram, i.e., relaxation time τ vs reciprocal measuring temperature $1/T$ for several of the observed processes. Upper data points: EAE results; lower data points: internal-friction results; \circ , $\langle 111 \rangle$ sample; Δ , $\langle 100 \rangle$ sample; \bullet , $\langle 110 \rangle$ sample, electron irradiation; \blacksquare , Ref. 7, α -particle irradiation; \blacktriangledown , Ref. 6, fast-neutron irradiation. The solid line for process B terminates at the temperature where a 10-min anneal would remove more than 99% of the defects.

irradiated and annealed simultaneously with the anelasticity sample. The recovery of the irradiation-induced resistivity changes is shown in Fig. 5. The values of n in Fig. 5 refer to the average number of interstitials per cluster present in the sample at various points of the annealing program. They were obtained from diffuse x-ray scattering experiments using samples with similar initial defect densities.²

III. DISCUSSION

In this section, the properties and possible origins of the anelastic processes are discussed in detail.

A. Process B

Process B is centered about 47 K in the EAE results for both crystal orientations (Figs. 2 and

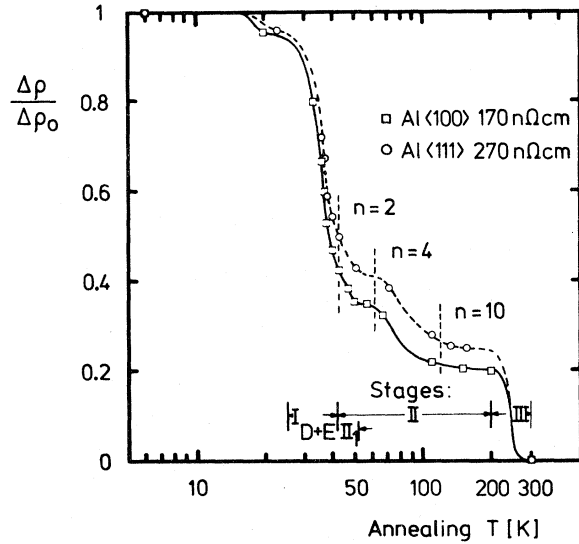


FIG. 5. Annealing of the resistivity changes measured at 6 K for both the $\langle 111 \rangle$ and $\langle 100 \rangle$ samples. The values of n refer to the average number of interstitials per cluster measured at the indicated points in the annealing program after a similar irradiation of aluminum by Ehrhart and Schilling (Ref. 2). The appropriate temperature intervals corresponding to the various annealing stages have also been marked.

3), but is absent from the internal-friction data (Fig. 1). Like process A,¹ it also anneals in the same temperature interval where the relaxation occurs, showing that defect reorientation occurs simultaneously with migration.

The temperature dependence of the relaxation time for process B yields

$$H = 0.135 \pm 0.25 \text{ eV and } \tau_0 = 3.4 \times 10^{-13 \pm 3} \text{ sec}$$

for the activation energy and preexponential time constant, respectively. These values readily explain the failure to observe process B in the internal-friction measurements. For the internal-friction pendulum operating at 40 Hz, Fig. 4 shows that the internal-friction peak maximum ($\tau \approx 10^{-2}$) for process B would be expected to occur near 70 K, well above the temperature (50 K) where the defects have already disappeared.

A comparison of the recovery of peak B (Fig. 3) with that of the resistivity (Fig. 5) reveals that the defect responsible for this process anneals in the temperature region slightly above stage I, called stage II₁. Huang scattering measurements² have shown that stage II₁ is primarily due to the disappearance of the di-interstitials present at the end of stage I. Therefore, process B is assigned to the simultaneous migration and reorientation of di-interstitials.

Assuming that the concentration of defects re-

sponsible for peak *B* is proportional to the initial defect concentration after irradiation, the ratio of the normalized relaxation strengths in the two different orientations is

$$\Delta^{\langle 100 \rangle} / \Delta^{\langle 111 \rangle} = 3.7 \pm 0.4.$$

This value indicates that the process *B* defect has lower than tetragonal symmetry, but not $\langle 100 \rangle$ orthorhombic.

Several years ago a model for the di-interstitial in fcc metals was proposed by Johnson on the basis of a computer calculation for copper.⁸ He found the most stable configuration to be that shown in Fig. 6. In this model, two parallel $\langle 100 \rangle$ -split interstitials sit on nearest-neighbor lattice sites. These sites lie along a $\langle 110 \rangle$ lattice direction perpendicular to the $\langle 100 \rangle$ interstitial axes. The defect symmetry is $\langle 110 \rangle$ orthorhombic. This di-interstitial possesses two different reorientation modes. In the first, motion of one of the single interstitials from configuration 1 to the equivalent arrangement 2 occurs through the metastable configuration 1'. This jump produces a 90° rotation of the $\langle 110 \rangle$ di-interstitial axis, and two-dimensional migration [in a $\langle 100 \rangle$ plane] of the defect center of mass. For the second mode, one of the dumbbells again migrates to 1', but then a rotation by 90° of the other interstitial occurs to stabilize the configuration. A 60° rotation of the $\langle 110 \rangle$ di-interstitial axis is produced, and migration of the center of mass occurs in three dimensions. As discussed by Nowick and Berry,⁵ $\langle 110 \rangle$ orthorhombic defects in cubic lattices possess two modes for reorientation. The relaxation time constants τ^c and $\tau^{c'}$, appropriate for the two shear elastic constants *C* and *C'*, are different. If ν_{ij} is the

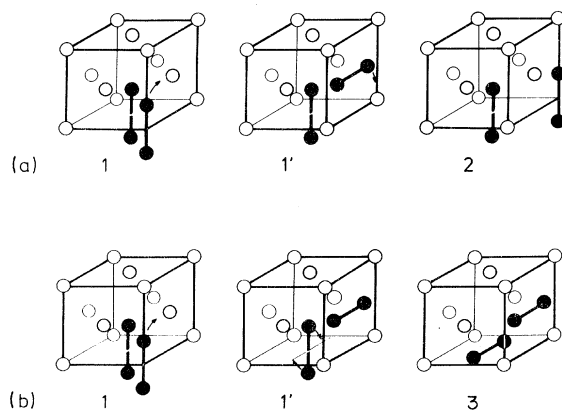


FIG. 6. Johnson di-interstitial configuration showing simultaneous reorientation and migration by (a) the mode with the lowest expected activation energy, and (b) the mode requiring a pure rotation of one of the interstitials and therefore a higher expected activation energy.

jump frequency for motion from configuration *i* into configuration *j*, the appropriate relaxation times are given by

$$1/\tau^{c'} = 6\nu_{13}$$

and

$$1/\tau^c = 2\nu_{12} + 4\nu_{13}.$$

The existence of two different relaxation modes suggests the possibility of observing two separate relaxation peaks, both due to di-interstitials. However, computer calculations^{8,9} suggest that the process 1 → 2 is much easier to excite than 1 → 3, i.e., the jump of a single interstitial to a nearest-neighbor site is energetically more favorable than a pure rotation. Hence only the 1 → 2 mode can be experimentally observed. The 1 → 3 mode would occur only at a much higher temperature. However, before this temperature can be attained experimentally, the vast majority of the di-interstitials have already disappeared during migration by the 1 → 2 mode. It follows that only the relaxation process described by

$$1/\tau^c = 2\nu_{12}$$

should be observed experimentally. This leads to an expected ratio of the relaxation strengths for the Johnson di-interstitial in aluminum of

$$\Delta^{\langle 100 \rangle} / \Delta^{\langle 111 \rangle} = 3.4.$$

Within experimental error, this is the value found for process *B*.

The assumption that just above stage I all the remaining residual resistivity change (Fig. 4) is due to di-interstitials and vacancies yields an upper limit for the concentration of di-interstitials present in the sample. This gives for the defect anisotropy,⁵ a value of

$$|P_{11} - P_{22}| \geq 6 \text{ eV}$$

and shows that the di-interstitial is considerably more anisotropic than a single interstitial.¹

All characteristics of process *B* can be understood in terms of the Johnson model for a di-interstitial. These results are therefore in agreement with diffuse x-ray scattering measurements on electron irradiated aluminum, in which evidence for this configuration was also found.¹⁰

B. Process 2

Process 2 appears in the internal-friction results (Fig. 1) near 42 K, well above the onset of long-range interstitial migration. Furthermore, the high-temperature side of the peak is distorted by annealing. The useful information pertaining to process 2 which is contained in the internal-fric-

tion measurements is therefore very limited. In the EAE measurements (Figs. 2 and 3), however, process 2 is found at 31 K. This lower observation temperature removes the complication of simultaneous annealing, as well as permits the relaxation strength of the process to be studied during stage I_{D+E} recovery. From Fig. 4, values of

$$H = 0.092 \pm 0.009 \text{ eV and } \tau_0 = 8 \times 10^{-14 \pm 1} \text{ sec}$$

are obtained for the activation energy and pre-exponential time constant, respectively.

In Fig. 7, the total relaxation strength observed at 31 K for process 2, and for comparison that of process B at 47 K, are plotted as a function of the annealing temperature for the two crystal orientations used in the EAE measurements. The relaxation strength is directly proportional to the

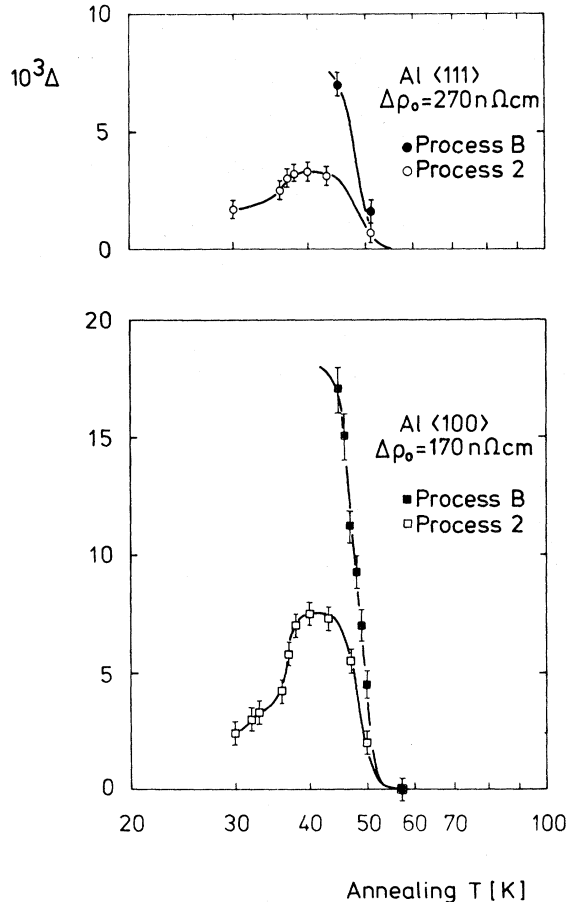


FIG. 7. Relaxation strengths of process B at 47 K and process 2 at 31 K as a function of the annealing temperature, for the $\langle 111 \rangle$ (above) and $\langle 100 \rangle$ (below) oriented samples. A change in the relaxation strength of a given anelastic process indicates a corresponding change in the concentration of defects responsible for that process.

concentration of the specific type of defect responsible for the anelastic process.⁵ Therefore, a change in the relaxation strength of a given anelastic process indicates a corresponding change in the concentration of defects responsible for that process. Process 2 begins to grow in strength in the annealing stage I_{D+E} and the increase is particularly sharp near the end of this stage. A few of the process 2 defects are apparently created during irradiation, but the primary mechanism for their production involves the long-range migration of interstitials which is known to occur between 30 and 45 K. Both process 2 and B disappear after annealing in stage II_1 , and furthermore, their annealing proceeds in a parallel fashion.

The reasoning behind the assignment of process B to the simultaneous migration and reorientation of Johnson di-interstitials was given in Sec. III A. Because of the similarity in recovery exhibited by processes 2 and B , an obvious interpretation would be the assignment of process 2 to a nonmigratory reorientation of this same defect. Such a separation of relaxation processes is not unknown, and is referred to in the literature as "frozen-free split."⁵ However, the previously cited model calculations, as well as experimental results,¹ indicate that a simple rotation of one of the interstitials requires considerably more energy to activate than the migration step, making the assignment of process 2 to the Johnson di-interstitial highly unlikely. A more probable explanation is that process 2 is due to a larger size cluster. The parallel annealing of processes B and 2 would then be explained by assuming either that both defects migrate simultaneously, or that only one type becomes mobile and reacts with a majority of the defects of the second type. In either case, the most likely candidate for the process 2 defect would appear to be the tri-interstitial.

Computer calculations^{9,11} indicate that the tri-SIA configuration shown in Fig. 8 may exist in fcc metals. This defect has nearly $\langle 110 \rangle$ orthorhombic symmetry, and is consistent with the observed ratio of the relaxation strengths in the two sample orientations. In addition, the computer calculations suggest that the middle dumbbell in this arrangement may rotate around the $\langle 100 \rangle$ axis connecting the two outer dumbbells with an activation energy less than that required for dissolution or migration of the defect. The rotation mode is shown in Fig. 8(c). Each single jump of the middle dumbbell leaves the defect configuration unaltered. Only the major axis of the defect dipole tensor undergoes rotation, and no long-range migration occurs. Thus a relaxation effect free from annealing is expected, in agreement with the experimental findings for process 2. It is therefore

possible to fully account for all the observed properties of process 2 in terms of the above model for the tri-interstitial. However, the possibility that a different tri-interstitial arrangement,¹¹ or even a somewhat larger size cluster, might be responsible for process 2 cannot be excluded on the basis of the present measurements. In any case, the simple model shown in Fig. 8 does account fully for all the observed properties of process 2. More generally, it provides a mechanism for explaining the observed relaxation of small interstitial clusters without any concomitant annealing.

C. Processes 0 and 4

In Sec. B, certain similarities were pointed out between processes 2 and *B*. Correlations also exist between two other processes, namely, 0 and 4. Process 0 appears in the internal-friction measurements near 6 K, the lowest attainable measuring temperature, and its true maximum probably occurs at an even lower temperature. It is the most easily activated of all the observed processes, and therefore, since it is buried in the instantaneous part of the strain recovery, does not appear in the isochronal EAE curves. Corresponding frequency measurements for process

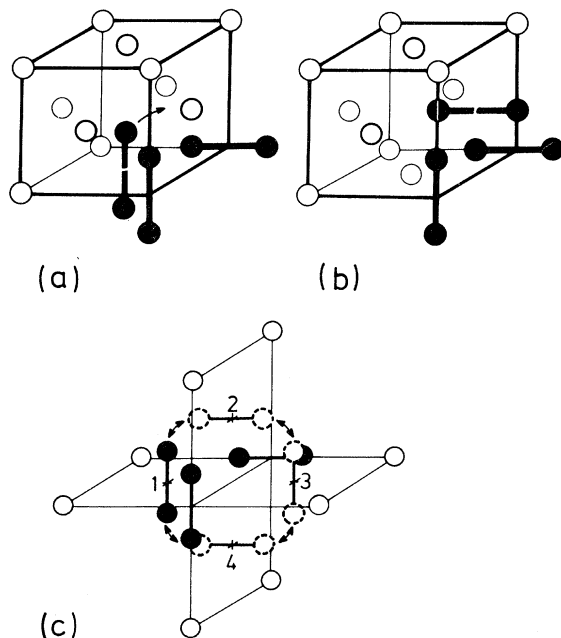


FIG. 8. Tri-interstitial configuration first proposed by Johnson. The different parts of the figure show how this defect may reorient by motion of the middle interstitial between four equivalent positions. This motion preserves the defect configuration, and does not result in long-range migration.

0 show it is indeed a true anelastic process, and not, as has been previously suggested,⁶ a consequence of helium droplets forming on the sample. However, because of the failure to observe a true peak maximum, no accurate values can be given for its activation energy and preexponential time constant.

Process 4 appears in both the internal-friction (Fig. 1, 58 K) and EAE (Figs. 2 and 3, 42 K) results. The behavior of its relaxation strength during the annealing program is shown in Fig. 9, along with that of process 0. The process-0 results shown here are internal-friction values measured at 6 K during the EAE experimental runs. The annealing of the relaxation strength for process A, which indicates the number of free SIA's remaining in the sample,¹ has also been included in Fig. 9. Particularly striking in Fig. 9 is the increase in concentration of process-0 defects as the free SIA's disappear. No significant number of process-0 defects are present either immediately after irradiation or below an annealing temperature of about 33 K (i.e., before any long-range defect migration has occurred). Their concentration grows from 33 through about 40 K, remains stable till approximately 60 K, and disappears completely in the 60–70-K annealing range. The growth and recovery pattern of process-0 defects exhibited in Fig. 9 is just that expected for a small interstitial cluster formed during long-range migration and reaction of single SIA's. The small cluster is stable over a limited temperature

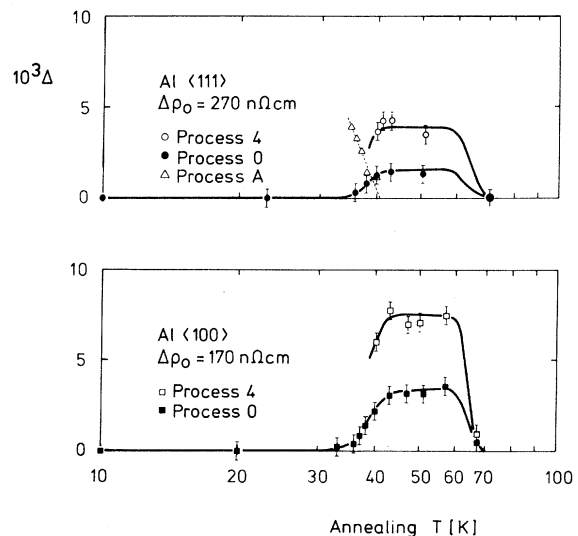


FIG. 9. Relaxation strengths of process 0 at 6 K and process 4 at 42 K as a function of the annealing temperature, for the $\langle 111 \rangle$ (above) and $\langle 100 \rangle$ (below) oriented samples. For comparison, the relaxation strength of process A (Ref. 1), which monitors the concentration of single SIA's present in the sample, is also shown.

range, and disappears at the point where thermal vibrations are sufficient to induce either its migration or disintegration. In the fast neutron study of Al,⁶ process 0 was observed immediately after irradiation below 5 K, a temperature well below that of free interstitial migration. Apparently, the cluster configuration responsible for process 0 is created in the displacement cascades produced by the large knock-on energies characteristic of fast neutrons.

The normalized relaxation strengths for the two processes 0 and 4 are within experimental error the same

$$\frac{\Delta_{\langle 100 \rangle}}{\Delta_{\langle 111 \rangle}} \Big|_0 = 3.4 \pm 0.7, \quad \frac{\Delta_{\langle 100 \rangle}}{\Delta_{\langle 111 \rangle}} \Big|_4 = 3.4 \pm 0.4.$$

Again, these values indicate a defect symmetry lower than tetragonal, but not $\langle 100 \rangle$ orthorhombic.⁵

For process 4, the measured activation energy and preexponential time constant are

$$H = 0.138 \pm 0.014 \text{ eV} \quad \text{and} \quad \tau_0 = 1.7 \times 10^{-15 \pm 1} \text{ sec.}$$

The simultaneous recovery of processes 0 and 4 suggests that they are caused by the same defect (see Sec. III A). Unfortunately, since even in the EAE results process 4 occurs at a temperature above stage I_{D+E} , it was impossible to observe its behavior during the onset of the long-range interstitial migration process. However, all indications are that it too is caused by a single type of small interstitial cluster, which if not the process-0 defect, is of approximately the same size. Since these processes show no change during annealing in stage II_1 , the responsible defects either do not possess a large cross section for reaction with, or they are present in much greater numbers than, the process 2 and B defects.

D. Process 1

Peak 1 appears in the internal-friction results (Fig. 1) near 20 K. Using the previously reported⁶ activation energy of approximately 30 meV, this process should appear at around 10 K in the EAE results, and indeed, a small effect of the correct order of magnitude is found there.

In both techniques, process 1 disappears after annealing of the sample in stage I_B , where the annihilation of a close-pair defect is known to occur. An anelastic process due to the I_B defect has also been reported in irradiated copper.¹²⁻¹⁴ That the situation for the stage- I_B defect is possibly more complex in Al is shown by the apparent existence of at least two more relaxation processes (Figs. 2 and 3, at 15 and 19 K) which also disappear after annealing in stage I_B . These latter two processes do not appear in the internal-fric-

tion results, because their internal-friction peaks would lie above the I_B annealing stage. It should be pointed out that the existence of so many relaxation modes for a close-pair defect might be considered surprising, but it is not unknown. Three have been observed for the I_C close pair in Ni.¹⁵

E. Processes 3 and 5

Both these processes result in very weak effects. Process 3 appears in the EAE results centered about 36 K. Combining the EAE and internal-friction measurements, it appears to anneal in the range from 70–110 K. Its small magnitude and the proximity of the much larger effects 2 and 4, obscure its behavior during stage I_{D+E} annealing. From Fig. 4, we obtain for process 3 values of

$$H = 0.105 \pm 0.010 \text{ eV} \quad \text{and} \quad \tau_0 = 10^{-13 \pm 1} \text{ sec.}$$

Process 5 occurs at 70 K in the internal-friction measurements, and anneals somewhere between 70 K and room temperature. Its weak relaxation strength made it impossible to identify in the EAE results. Because of the temperature range in which these two processes disappear, they too are apparently due to the reorientation of small interstitial clusters. Their weak relaxation strengths show that the concentration of these particular size clusters and/or their elastic anisotropies are small.

After annealing at 110 K, no anelastic processes are present in the temperature range from 6 to 60 K. This observation is in agreement with diffuse x-ray scattering measurements,² which show that by this point in the annealing program the interstitial clusters have collapsed to form dislocation loops.

IV. SUMMARY

Several anelastic processes arising from the stress-induced ordering of self-interstitial defects produced by low-temperature electron irradiation and annealing of aluminum have been observed. Process 1 is due to the I_B close-pair defect, while six others, labeled 0, 2, 3, 4, 5, and B are caused by small interstitial clusters formed during the long-range migration and interaction of interstitials in and above recovery stage I_{D+E} . Process B was observed only during defect migration in recovery stage II_1 . Its symmetry, annealing properties, and large anisotropy (> 6 eV) all support an interpretation in terms of the simultaneous migration and reorientation of Johnson di-interstitials. The other five processes are all stable, indicating that they are due to a simple defect rotation involving one or more members of a cluster, which results in no long-range migration of

the defect center of mass. A model based on computer studies by Schober¹¹ of a tri-interstitial configuration has been presented which suggests how a simple rotation of a small interstitial cluster may occur.

A definite advantage offered by anelastic measurements to the study of interstitial clustering is the ability to discriminate between various cluster configurations present simultaneously in the sample. Each relaxation process corresponds to a specific type of defect, and is not an effect averaged in some manner over all cluster configurations present in the sample. The combination of two quite different techniques, EAE and internal friction, which were employed here for studying anelastic effects has proven quite useful. In the case of stable processes, internal friction provides a high degree of sensitivity, permitting the detection of even very weak effects. Since the EAE technique allows processes to be observed at temperatures where defect jumps occur only about once every 100 sec, it permits observation of defect reorientation during migration, as well

as creates the largest possible separation between the peak temperature of a stable relaxation process and its annealing temperature. This large separation made it possible to observe the formation of specific cluster types during long-range interstitial migration in stage I, as well as their disappearance in stage II. In addition to the simple summation of the advantages offered by each technique taken separately, the appearance of an effect in both provides a measurement of the defect relaxation time over about five orders of magnitude, furnishing a very accurate description of the thermodynamics of the process.

ACKNOWLEDGMENTS

The authors would like to thank Dr. P. H. Dederichs and Dr. H. R. Schober for many helpful discussions. The technical assistance of Frau I. Serpekian is also gratefully acknowledged. We thank Dr. F. W. Young, Jr. for a careful reading and discussion of the manuscript.

*Present address: Materials Science Division, Argonne National Laboratory, Argonne, Ill. 60439.

¹V. Spirić, L. E. Rehn, K.-H. Robrock, and W. Schilling, preceding paper, *Phys. Rev. B* **15**, 672 (1977).

²P. Ehrhart and W. Schilling, *Phys. Rev. B* **8**, 2604 (1973).

³K.-H. Robrock, Report of the Kernforschungsanlage, Jülich, Germany, Report No. Jül-1088-FF, 1974 (unpublished).

⁴J. Hemmerich, Report of the Kernforschungsanlage, Jülich, Germany, Report No. Jül-579-FN, 1969 (unpublished).

⁵A. S. Nowick and B. S. Berry, *Anelastic Relaxation in Crystalline Solids* (Academic, New York, 1972).

⁶K. Ehrensberger, V. Fischer, J. Kerscher, and H. Wenzl, *J. Phys. Chem. Solids* **31**, 1835 (1970).

⁷M. Riggauer, W. Schilling, J. Völkl, and H. Wenzl,

Phys. Status Solidi **33**, 843 (1969).

⁸R. A. Johnson, *J. Phys. Chem. Solids* **26**, 75 (1965); *Phys. Rev.* **152**, 629 (1966).

⁹P. H. Dederichs, C. Lehmann, and A. Scholz, *Phys. Rev. Lett.* **31**, 1130 (1973).

¹⁰P. Ehrhart, H.-G. Haubold, and W. Schilling, *Adv. Solid State Phys.* **XIV**, 87 (1974).

¹¹H. R. Schober (unpublished).

¹²R. L. Nielsen and J. R. Townsend, *Phys. Rev. Lett.* **21**, 1749 (1968).

¹³J. Holder, A. V. Granato, and L. E. Rehn, *Phys. Rev. B* **10**, 363 (1974).

¹⁴A. V. Granato, in *Fundamental Aspects of Radiation Damage in Metals*, edited by M. T. Robinson and F. W. Young (U. S. A. ERDA Conf.-751006, 1976).

¹⁵G. de Keating-Hart, R. Cope, C. Minier, and P. Moser, *Jülich-Conf.* **1**, 327 (1968).